and one reoxidizable species exist whether excess ligand is present or not. Hence, **2** must be fully ligated in both the ferric and ferrous states. Species **1**, on the other hand, undergoes partial ligand dissociation upon reduction, resulting in formation of some five-coordinate $Fe^{II}TPP(4MeIm)^-$. The fully formed, six-coordinate complex, $Fe^{II}TPP(4MeIm)_2^{2-}$ can thus only be observed in the presence of excess ligand. Relatively low ligand affinities of ferrous porphyrin imidazolate complexes have also been observed by other investigators.[11] In the present case, the large negative charge on the reduced six-coordinate complex may be responsible for the low affinity for the second imidazolate ligand.

Finally, comparison of $E_{1/2}$ of **2** and $^1/_2(E_{pc} + E_{pa})$ of **1** reveals that deprotonation results in an approximately 700-mV stabilization of the ferric state. Undoubtedly, a substantial portion of this effect is due to the charges of the species being reduced (i.e., **1** is an anion; **2** is a cation).

Acknowledgment. Financial support from the USPHS (Grant GM 28222 to J.S.V.), a BRSG grant (J.S.V.), and the NSF (C.E.S.) is gratefully acknowledged. R.Q. was the recipient of a Johnson and Johnson fellowship in chemistry administered by Rutgers University. We also thank Dr. C. Knobler and N. Keder for helpful discussions.

Registry No. **1**, 87494-49-3; $Fe(TPP)(4\text{-}MeImH)_2SbF_6$, 80939-26-0; $Fe(TPP)(SbF_6)$, 79949-97-6; Fe(TPP)Cl, 16456-81-8; Fe(TPP)(4-MeIm), 80925-73-1.

Supplementary Material Available: Calculated hydrogen atom positions (Table VIII), isotropic thermal parameters (Table IX), anisotropic thermal parameters (Table X), and a listing of observed and calculated structure factors (20 pages). Ordering information is given on any current masthead page.

Contribution from the Department of Chemistry and Materials and Molecular Research Division, Lawrence Berkeley Laboratory, University of California, Berkeley, California 94720

Specific Sequestering Agents for the Actinides. 9. Synthesis of Metal Complexes of 1-Hydroxy-2-pyridinone and the Crystal Structure of Tetrakis(1-oxy-2-pyridonato)aquothorium(IV) Dihydrate[1]

PAUL E. RILEY, KAMAL ABU-DARI,[2] and KENNETH N. RAYMOND*

Received April 1, 1983

The Zr(IV), Ce(IV), Th(IV), and U(IV) complexes of 1-oxy-2-pyridonate ($C_5H_4NO_2^-$) have been prepared, and the crystal structure of the dihydrate of the nine-coordinate complex $(C_5H_4NO_2)_4(H_2O)Th$ has been determined by single-crystal X-ray diffraction techniques with data obtained by counter methods. The Th(IV) complex consists of neutral molecules of rigorous C_2 symmetry in which Th(IV) and the coordinated water molecule lie along the C_2 axis parallel to *b*. The immediate coordination sphere about Th is completed by the eight oxygen atoms of the four bidentate $C_5H_4NO_2^-$ ligands [average r(Th–O) = 2.44 Å] and the water molecule [r(Th–O) = 2.52 Å], such that the resulting nine-coordinate complex resembles a D_{3h} tricapped trigonal prism, although the actual geometry is an intermediate nearly on the C_{2v} symmetry pathway between the C_{4v} monocapped Archimedean antiprism and the D_{3h} tricapped trigonal prism. The difference betweeen this structure and the similar nine-coordinate tetrakis(tropolonato)(*N*,*N*-dimethylformamide)thorium(IV) complex, which is closer to the C_{4v} structure, is explained as largely due to the asymmetric charge distribution in the oxypyridinone ligand as compared with tropolonate. The compound crystallizes as colorless parallelepipeds in the orthorhombic space group *Pbcn* with *a* = 12.880 (1) Å, *b* = 8.812 (2) Å, and *c* = 20.826 (2) Å. The calculated density (2.04 g cm^{-3}) agrees well with the measured value (2.04 g cm^{-3}) and is consistent with four formula units of the dihydrate per unit cell. Full-matrix least-squares refinement of the structure with use of the 2100 reflections with $F_o^2 > 3\sigma(F_o^2)$ has converged with R and R_w indices of 0.026.

Introduction

We have previously noted that the coordination chemistry of actinide(IV) ions is in some ways markedly similar to that of iron(III), and we have used this similarity to design highly specific actinide(IV) sequestering agents.[1,3] Incorporated into such synthetic macrochelating ligands have been those groups, principally catecholate and hydroxamate, that are known to bind iron(III) strongly in the bacterial iron transport and chelating agents called siderophores.

A detailed assessment of the architecture of the simple prototypical complexes formed between actinide(IV) ions and these small groups is particularly important if the desired synthetic macrochelating ligands are to be suitably designed to fulfill more satisfactorily—and hence more specifically—the coordination requirements of a particular actinide(IV) ion. Accordingly we have recently reported[3] the synthesis and the crystal structures of two eight-coordinate Th(IV) complexes of the bidentate hydroxamate ligands

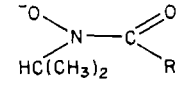

R = $CH_2C(CH_3)_3$, $C(CH_3)_3$

We have now extended this work by preparing metal complexes of the related bidentate ligand 1-oxy-2-pyridonate ($C_5H_4NO_2^-$)

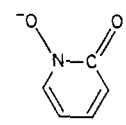

which in one view represents a slight variation of the common hydroxamate ligand depicted above and in another is iso-

* To whom correspondence should be addressed at the Department of Chemistry.

(1) Previous paper in this series: Abu-Dari, K.; Raymond, K. N. *Inorg. Chem.* **1982**, *21*, 1676.
(2) On leave from the Chemistry Department, University of Jordan, Amman, Jordan.
(3) Smith, W. L.; Raymond, K. N. *J. Am. Chem. Soc.* **1981**, *103*, 3341 and references therein.

0020-1669/83/1322-3940$01.50/0

Table I. Analytical Results[a]

complex	color	% calcd				% found			
		C	H	N	metal	C	H	N	metal
$(C_5H_4NO_2)_4Zr\cdot CHCl_3$	white	38.75	2.63	8.60	14.0	40.51	3.00	8.63	16.0
$(C_5H_4NO_2)_4Ce\cdot H_2O$	red	39.83	2.77	9.13		40.13	3.00	9.36	
$(C_5H_4NO_2)_4Th\cdot H_2O$	colorless	34.79	2.62	8.11		35.00	2.54	7.85	
$(C_5H_4NO_2)_4U\cdot CHCl_3$	blue-green	31.62	2.15	7.02	29.8	32.25	2.24	7.25	31.2

[a] Microanalyses were performed by Analytical Services, Department of Chemistry, University of California, Berkeley, CA. Analyses for metal content were carried out locally by atomic absorption spectroscopy.

Table II. Crystallographic Summary for $(C_5H_4NO_2)_4(H_2O)Th\cdot 2H_2O$[a]

a, Å	12.880 (1)	space group	*Pbcn* (No. 60)
b, Å	8.812 (2)	mol formula	$C_{20}H_{22}N_4O_{11}Th$
c, Å	20.826 (2)	fw	726.46
V, Å^3	2363.7 (4)	*Z*	4
2θ range for cell const, deg	18.2–20.5	d_{measd},[b] g cm^{-3}	2.04
cryst syst	orthorhombic	d_{calcd}, g cm^{-3}	2.041
systematic reflcn absences	$0kl$, $k = 2n + 1$ $h0l$, $l = 2n + 1$ $hk0$, $h + k = 2n + 1$	$F(000)$, e	1392
2θ range for data collection, deg	3.0–70.0	data cryst faces	(100), ($\bar{1}$00) (011), (0$\bar{1}\bar{1}$) (01$\bar{1}$), (0$\bar{1}$1)
total reflcns measd	5188	abs coeff, (μ(Mo Kα)), cm^{-1}	65.8
check reflcns	no decay over 95 h of data collection	transmission factor range[c]	0.39–0.63
data cryst dimens, mm	0.08 × 0.18 × 0.18		

[a] Numbers in parentheses are the estimated standard deviations in the last significant digit. [b] Flotation at 20 °C in a $CHBr_3/CCl_4$ mixture. [c] Examination of six reflections with $\chi = 90 \pm 10°$ at approximately regular intervals ($\Delta 2\theta = 5°$) in reciprocal space for $10 < 2\theta < 37°$ by the ψ-scan technique revealed an appreciable variation in normalized transmission factors (0.64–1.00), thereby suggesting the need for an absorption correction.

electronic with the catecholate anion (N substituting for C in the ring). In this paper, we report the synthesis of the Zr(IV), Ce(IV), Th(IV), and U(IV) complexes of this ligand and the crystal structure of the dihydrate of the $(C_5H_4NO_2)_4(H_2O)Th$ complex; these structural data will be used in our continuing design and refinement of actinide-specific macrochelate sequestering agents.

Experimental Section

Materials. The compounds obtained from commercial sources were as follows: 1-hydroxy-2-pyridinone from Aldrich Chemical Co., anhydrous UCl_4 and $ThCl_4\cdot 8H_2O$ from ROC–RIC Research Chemical Corp., $(NH_4)_4Ce(SO_4)_4\cdot 2H_2O$ from J. T. Baker Chemical Co., and aqueous $Zr(NO_3)_4$ from Alfa Products. All materials were used as supplied without further purification. The reaction with UCl_4 was conducted under dry argon by using Schlenk-line techniques with degassed aqueous solutions. However, unlike the hydroxamate complexes of U(IV) studied earlier,[3] the resulting complex was air stable and decomposed to red UO_2^{2+} only after prolonged exposure to air (unlike the oxygen abstraction from the hydroxamate ligands).[3]

Tetrakis(1-oxy-2-pyridonato)aquothorium(IV). A solution of 1.11 g (10 mmol) of 1-hydroxy-2(1*H*)-pyridinone in 10 mL of aqueous 1 M NaOH was added slowly with stirring to 20 mL of an aqueous solution of 1.30 g (2.5 mmol) of $ThCl_4\cdot 8H_2O$. A clear solution was obtained, which, with additional stirring, afforded a white precipitate. This white material was removed by filtration, washed several times with water to remove unreacted $ThCl_4\cdot 8H_2O$ and ligand, and dried in vacuo over P_2O_5.

The preparations of the Zr(IV), Ce(IV), and U(IV) complexes were carried out as described for the Th(IV) species, except that the synthesis of the U(IV) complex was subject to the conditions cited above. All materials were recrystallized in air from chloroform–ethanol mixtures. Analytical data for all compounds are given in Table I.

Attempts to obtain single crystals suitable for X-ray diffraction studies were successful only for the Th(IV) complex, which was recrystallized from a 1:1 mixture of $CHCl_3$ and 95% C_2H_5OH. Precession photographs of a colorless parallelepiped, which had been wedged into a thin-walled capillary, displayed orthorhombic symmetry and systematic absences consistent with space group *Pbcn*. Preliminary examination of the data crystal with an Enraf-Nonius CAD 4 automated diffractometer confirmed the space group and cell constants and demonstrated that the crystal was of good quality. The crystal mosaicity (measured from peak widths at half-peak heights), as determined by ω-scans with a receiving aperture of 1-mm width, was ~0.20° for intense, low-angle reflections. Accurate cell constants were determined from the refinement of 25 accurately centered high-angle reflections selected from diverse regions of reciprocal space; intensity data were collected, reduced, corrected for absorption, and assigned standard deviations (with $p = 0.02$) in accordance with previously published procedures.[4,5] Crystal data and those variables of data collection that are peculiar to this study are presented in Table II.

The structure was solved by standard heavy-atom procedures and refined by full-matrix least-squares methods[6] using reflections with $F_o^2 > 3\sigma(F_o^2)$. The function minimized in refinement was $\sum w(|F_o| - |F_c|)^2$.[7] Neutral-atom scattering factors for Th, O, N, C, and H, corrected for the anomalous scattering of Mo Kα radiation, were used in these calculations.[5] Full-matrix least-squares refinement of the structure, in which the thermal motion of non-hydrogen atoms was treated anisotropically, converged with $R = 0.026$, $R_w = 0.026$, and an error in an observation of unit weight of 1.18[8] for 2100 reflections and 165 variables. Hydrogen atoms of the ligand (located from a difference electron density map) were fixed at idealized positions[9] and assigned fixed isotropic thermal parameters of 5.0 Å^2, while those of the water molecules were not located. Distinction of the N atoms of the pyridinone rings was initially made from thermal parameters (with all atoms assigned as carbon) and subsequently confirmed from the final structure. Comparison of $|F_o|$ vs. $|F_c|$ indicated that the data were affected by secondary extinction; hence, a small correction [2.9 (3) × 10^{-8} e^{-2}] for this effect was included in the concluding cycles of refinement. In the final cycle of refinement, all shifts in parameters were less than 0.07 of a corresponding estimated standard deviation (esd). The largest peaks on a final difference Fourier map were 0.3–0.5

(4) Abu-Dari, K.; Raymond, K. N. *Inorg. Chem.* **1980**, *19*, 2034.
(5) Eigenbrot, C. W., Jr.; Raymond, K. N. *Inorg. Chem.* **1982**, *21*, 2653.
(6) The computer program package used in this work is cited in ref 5.
(7) The weight w used in refinement is $4F_o^2/\sigma^2(F_o^2)$ (the reciprocal square of the standard deviation of each observation $|F_o|$).
(8) The error indices are $R = \sum||F_o| - |F_c||/\sum|F_o|$ and $R_w = [\sum w(|F_o| - |F_c|)^2/\sum w|F_o|^2]^{1/2}$, and the error in the observation of unit weight = $[\sum w(|F_o| - |F_c|)^2/(N_o - N_v)]^{1/2}$, where N_o is the number of observations $|F_o|$ and N_v is the number of variables in refinement.
(9) The C–H bond lengths were constrained to 0.95 Å in accordance with a previous study: Churchill, M. R. *Inorg. Chem.* **1973**, *12*, 1213.

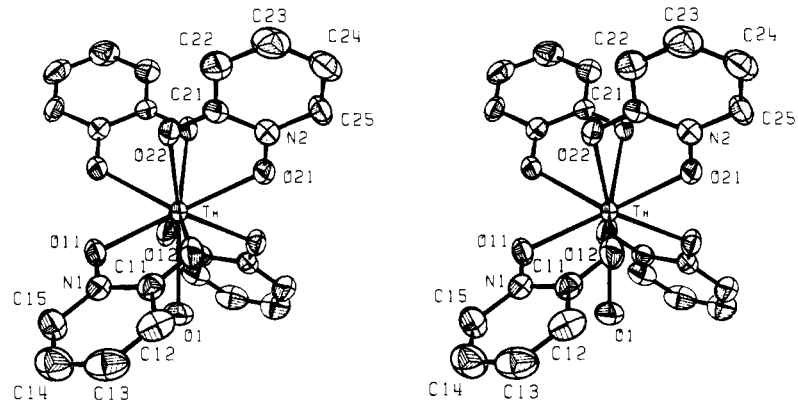

Figure 1. Stereoscopic view of $(C_5H_4NO_2)_4(H_2O)Th$, illustrating the atom-numbering scheme. Atoms are drawn as ellipsoids of 50% probability; hydrogen atoms have been omitted for clarity. A crystallographic C_2 axis is coincident with the Th–O(1) bond (vertical axis) and thus carries the left and right halves of the molecule into each other.

Table III. Fractional Coordinates of Non-Hydrogen Atoms[a]

atom	x	y	z
Th	0.0000 (0)	0.09845 (2)	0.2500 (0)
O(11)	0.1570 (2)	−0.0015 (4)	0.2017 (2)
O(12)	−0.0143 (2)	0.0143 (4)	0.1372 (2)
O(21)	0.1552 (2)	0.2146 (4)	0.2882 (2)
O(22)	−0.0237 (2)	0.3241 (4)	0.3198 (2)
O(1)	0.0000 (0)	−0.1878 (5)	0.2500 (0)
O(2)	0.1342 (3)	−0.4086 (4)	0.2268 (2)
N(1)	0.1502 (3)	−0.0772 (4)	0.1452 (2)
N(2)	0.1515 (3)	0.3236 (5)	0.3328 (2)
C(11)	0.0587 (4)	−0.0644 (6)	0.1121 (3)
C(12)	0.0542 (5)	−0.1390 (7)	0.0526 (3)
C(13)	0.1362 (6)	−0.2233 (7)	0.0299 (3)
C(14)	0.2249 (5)	−0.2373 (7)	0.0666 (3)
C(15)	0.2306 (4)	−0.1629 (6)	0.1231 (3)
C(21)	0.0570 (4)	0.3790 (5)	0.3496 (3)
C(22)	0.0522 (4)	0.4938 (7)	0.3952 (3)
C(23)	0.1404 (6)	0.5488 (7)	0.4219 (3)
C(24)	0.2373 (5)	0.4922 (7)	0.4038 (3)
C(25)	0.2410 (4)	0.3804 (6)	0.3592 (3)

[a] See Figure 1 for identity of the atoms. Numbers in parentheses are the estimated standard deviations in the least significant digits.

e Å^{-3} and were within 0.8 Å of the Th position or the water molecule [O(1)] bonded to Th. For comparison, the water molecules of this structure had heights of 3.2 and 5.2 e Å^{-3} on a previous difference Fourier map. Examination of $|F_o|$ vs. $|F_c|$ at the end of refinement showed no trends as a function of $|F_o|$, $(\sin\theta)/\lambda$, or Miller index.[10]

Table III presents the positional parameters of the non-hydrogen atoms with esd's as derived from the least-squares inverse matrix. Tabulations of anisotropic thermal parameters (Table IV), hydrogen atom parameters (Table V), and observed and calculated structure factor amplitudes (Table VI) are available.[11]

Discussion

Figure 1 provides a stereoscopic view of the molecule and indicates the atom-numbering scheme used herein. Selected bond lengths and bond angles are given in Table VII, and selected mean planes, in Table VIII.[11]

The crystal structure of $(C_5H_4NO_2)_4(H_2O)Th\cdot 2H_2O$ consists of neutral molecules of rigorous C_2 symmetry in which the Th^{4+} ions and the oxygen atoms of the coordinated H_2O molecules [O(1)] lie along the crystallographic twofold axes parallel to *b*. The immediate thorium coordination sphere is completed by the eight oxygen atoms of the four bidentate oxypyridinone ligands, such that the resulting nine-coordinate

(10) This analysis was made with the FORTRAN program REVAL, written locally by F. J. Hollander.
(11) Supplementary material.

Table VII. Selected Bond Lengths (Å) and Bond Angles (deg) for $(C_5H_4NO_2)_4(H_2O)Th\cdot 2H_2O$[a]

Th–O(11)	2.424 (3)	Th–O(22)	2.482 (4)
Th–O(12)	2.469 (4)	O(21)–N(2)	1.336 (5)
O(11)–N(1)	1.356 (5)	O(22)–C(21)	1.303 (6)
O(12)–C(11)	1.281 (6)	N(2)–C(21)	1.358 (6)
N(1)–C(11)	1.371 (6)	C(21)–C(22)	1.390 (7)
C(11)–C(12)	1.403 (8)	C(22)–C(23)	1.354 (8)
C(12)–C(13)	1.375 (8)	C(23)–C(24)	1.396 (9)
C(13)–C(14)	1.380 (9)	C(24)–C(25)	1.355 (7)
C(14)–C(15)	1.348 (9)	C(25)–N(2)	1.372 (6)
C(15)–N(1)	1.361 (7)	O(11)···O(12)	2.587 (5)
Th–O(1)	2.522 (4)	O(21)···O(22)	2.582 (4)
Th–O(21)	2.382 (3)		
O(11)–Th–O(12)	63.8 (1)	O(1)–Th–O(21)	115.4 (1)
O(11)–Th–O(22)′	86.9 (1)	O(21)–Th–O(21)′	129.1 (2)
O(12)–Th–O(22)′	72.1 (1)		

[a] Numbers in parentheses are the estimated standard deviations in the least significant digits. See Figure 1 for identity of the atoms. Coordinates of primed atoms are related to the correspondingly numbered atoms of Table III by the C_2 transformation $\bar{x}, y, {}^1/_2 - z$.

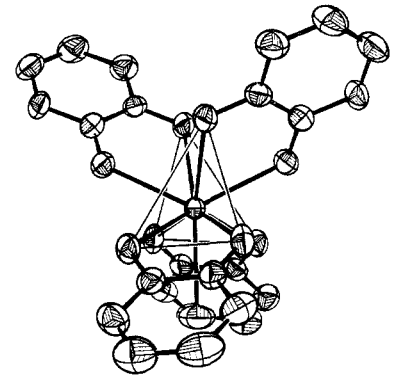

Figure 2. View normal to the plane formed by the vectors along the Th–O(1) bond and the O(21) to O(21)′ direction, i.e., approximately along the pseudo-C_3 axis of the molecule. The C_2 symmetry axis is still vertical; this view is rotated clockwise around the C_2 axis relative to that in Figure 1. Atoms are drawn as ellipsoids of 50% probability, and hydrogen atoms have been excluded for clarity.

complex resembles a D_{3h} tricapped trigonal prism (see below). Both hydrogen atoms of the coordinated water molecule [bound to O(1) and equivalent by C_2 symmetry] are hydrogen bonded to water molecules [O(2)] that lie off the C_2 axis. These molecules in turn are hydrogen bonded to one of the two carbonyl [O(22)] atoms, which are related by the C_2 axis and which define one of the polyhedral edges, which is approximately parallel to the pseudo C_3 axis of the distorted D_{3h} polyhedron (see Figure 2). In addition, each O(2) water

Table IX. Comparison of Dihedral Angles δ (deg) of $(C_5H_4NO_2)_4(H_2O)Th$ to Those of the Idealized D_{3h} and C_{4v} Polyhedra[a]

type of faces	position	idealized δ	face 1[b]	face 2[b]	determined δ
		D_{3h} Tricapped Trigonal Prism			
opposed (⊥)	⊥ threefold axis	180	O(11), O(22)′, O(12)	O(12)′, O(22), O(11)′	159.2
opposed (∥)	∥ threefold axis	146.4	O(21), O(22)′, O(22)	O(1), O(11)′, O(12)	149.5
			O(21), O(12)′, O(11)	O(21)′, O(11)′, O(12)	130.8
			O(1), O(12)′, O(11)	O(21)′, O(22), O(22)′	149.5
vicinal (∥)	∥ threefold axis	26.4	O(21), O(22)′, O(22)	O(21)′, O(22), O(22)′	49.0
			O(21)′, O(11)′, O(12)	O(1), O(11)′, O(12)	12.5
			O(1), O(12)′, O(11)	O(21), O(12)′, O(11)	12.5
		C_{4v} Monocapped Square Antiprism			
opposed	1 vertex on square face	163.5	O(21)′, O(11)′, O(12)	O(21), O(11), O(12)′	130.8
			O(12)′, O(11)′, O(22)	O(11), O(12), O(22)′	159.2
opposed	2 vertices on square face	138.2	O(21)′, O(11)′, O(22)	O(21), O(11), O(22)′	132.0
			O(21), O(12)′, O(22)	O(21)′, O(22)′, O(12)	139.1
vicinal (⊥)	⊥ fourfold axis	0	O(21), O(22), O(22)′	O(21)′, O(22), O(22)′	49.0

[a] Shape-determining dihedral angles for these idealized polyhedra and definition of face type are given in ref 13. [b] See Figure 1 for identity of atoms. Primed atoms are related to the positions of the correspondingly numbered unprimed atoms of Table III by the C_2 transformation $\bar{x}, y, {}^1/_2 - z$.

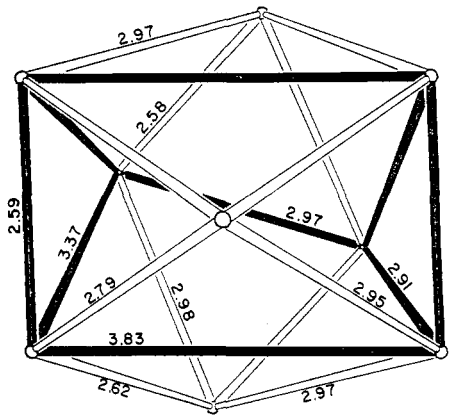

Figure 3. Perspective view of the coordination polyhedron down the C_2 axis. The C_3 axis of the D_{3h} tricapped trigonal prism to which this geometry relatively closely conforms is horizontal in this view, such that the view direction is one of the three rectangular caps of the trigonal prism. Atom O(11) is at the lower left vertex of the front rectangular array, and O(21) is the uppermost vertex in the diagram.

molecule is hydrogen bonded to an O(11) atom of an adjacent polyhedron, thereby linking all of the molecules of the structure together.

The views of the coordination polyhedron in Figures 1–3 show various aspects of the relationship of this geometry to the nine-coordinate high-symmetry polyhedra: the C_{4v} monocapped Archimedean antiprism and the D_{3h} tricapped trigonal prism. In both Figures 1 and 2 the vertical axis is the C_2 axis of the complex, which would be the C_4 axis of the C_{4v} geometry and would be one of the dihedral C_2 axes of the D_{3h} geometry. The actual geometry is closest to the C_{2v} reaction path that is the highest symmetry that can be maintained while interconverting the C_{4v} and D_{3h} geometries. Figure 3 shows a view down the C_2 axis that illustrates the degree to which this structure is distorted from C_{2v} symmetry.

With respect to the C_{4v} polyhedron, if the lower cap is the "bottom" of the molecule, as seen in both Figures 1 and 2, the arrays of oxygen atoms that would correspond to the two squares of the Archimedean antiprism can be referenced to this. It can be seen that the four oxygen atoms (O(11), O(12), O(11)′, and O(12)′) from the lower pair of C_2-related pyridinone rings are nearly planar and hence form a rectangle. This planarity is presented quantitatively in Table VIII.[11] The rectangle, which would be a square in the C_{4v} geometry, is 2.59 Å along the chelate "bit" edge and 3.83 Å between rings (i.e., O(11) and O(12)′), as shown in Figure 3. As a result of this distortion of the bottom square array to a rectangle, the upper square array (the rear four vertices in Figure 3—atoms O(21), O(22), O(21)′, and O(22)′) sees less repulsion toward the top and bottom of the polyhedron (as shown in Figure 3) compared to left and right. Hence, what would be the upper square array of the C_{4v} geometry folds across its diagonal (the 2.97-Å edge through which the C_2 axis passes) to give two trigonal faces and the polyhedron shown in Figure 3. In summary, this structure can be viewed in relation to the C_{4v} Archimedean antiprism by distorting the square-capped plane to a rectangle. The result is a C_{2v} geometry with one new face. This C_{2v} geometry is an intermediate between the C_{4v} Archimedean antiprism and the D_{3h} tricapped trigonal prism. The actual C_2 symmetry is a further distortion from the C_{2v} polyhedron.

A direct comparison of this structure can be made with the corresponding nine-coordinate complex tetrakis(tropolonato)(*N*,*N*-dimethylformamide)thorium(IV).[12] Like the structure reported here, the tropolonato compound is also a tetrakis(bidentate)–mono(monodentate) complex in which all of the ligating atoms are oxygen. In both structures, the Th–O neutral ligand distances are 2.52 Å and the average Th–O bidentate anion distances are 2.44 Å. However, the tropolonato complex conforms to a coordination polyhedron that more closely approximates the C_{4v} monocapped Archimedean antiprism, while the oxypyridinone complex is closer to the D_{3h} tricapped trigonal prism. In the tropolonato complex the actual coordination symmetry is approximately C_s, since the chelate ligands are arrayed such that one provides the cap oxygen, one bridges an edge of a square face of the antiprism, and two bridge between the upper and lower square atom arrays. As the authors of the tropolonato paper[12] point out, this is not a distortion that represents a pathway to the D_{3h} tricapped trigonal prism.

In the oxypyridinone structure reported here, the dihedral angle shape parameters[13] (Table IX) clearly conform more closely to the D_{3h} tricapped trigonal prism than to the C_{4v} monocapped Archimedean antiprism. As noted earlier, the actual geometry is only slightly distorted from the C_{2v} structure that is on the highest symmetry pathway between the C_{4v} monocapped Archimedean antiprism and the D_{3h} tricapped trigonal prism geometries.[14] (This is presented quantitatively in Table X.) One trigonal edge of the top and bottom faces of the trigonal prism is bridged by oxypyridinone ligands. Two caps are formed by oxypyridinone nitroso oxygen atoms and the third by the water molecule. As a result, the more neg-

(12) Day, V. W.; Hoard, J. L. *J. Am. Chem. Soc.* **1976**, *92*, 3626.
(13) Guggenberger, L. J.; Muetterties, E. L. *J. Am. Chem. Soc.* **1976**, *98*, 7221.
(14) For a detailed discussion of nine-coordinate polyhedra and a review of known nine-coordinate structures see: Kepert, D. L. "Inorganic Stereochemistry"; Springer Verlag: New York, 1982.

Table X. Deviations from the Symmetry Plane of an Idealized C_{2v} Polyhedron[a]

atom	displacement, Å	atom	displacement, Å
O(11)	−1.269 (4)	O(12)	1.313 (4)
O(22)	−0.447 (4)	O(22)′	0.447 (4)

atoms[b]	torsion angle, deg
O(12)′, MID2, MID1, O(11)	2.6
O(11)′, MID2, MID1, O(12)	2.6
O(22), MID2, MID1, O(22)′	19.1

[a] Pseudo symmetry plane formed by atoms Th and O(1) and the point between O(11) and O(12), which yields the plane which is normal to the O(11)–O(12)–O(11)′–O(12)′ least-squares plane. Coordinates of primed atoms are related to the correspondingly numbered atoms of Table III by the C_2 transformation $\bar{x}$, y, $^1/_2 - z$. [b] MID1 and MID2 represent the centroids of the opposing faces formed by [O(11), O(12), O(22)′] and [O(12)′, O(11)′, O(22)].

atively charged NO groups are arrayed symmetrically and are farther apart than would be possible in the C_{4v} geometry. While the larger O–O bite distance of the oxypyridinonate (2.58 Å) compared to tropolonate (2.53 Å) rings may be significant, it seems probable that the asymmetry of the negative charge distribution of the oxypyridinonate compared to tropolonate rings is the major factor in the difference in structure of their nine-coordinate thorium complexes.

Comparison of the effect of ligand-charge asymmetry on Th–O bond length can be made with the structures of the two eight-coordinate hydroxamate complexes of Th^{4+} described earlier. In these aliphatic hydroxamate compounds the Th–O_N bonds are 0.10 and 0.14 Å shorter than the Th–O_C bonds. In the nine-coordinate complex reported here, this difference is less pronounced (~0.07 Å, see Table VII) and thus is consistent with a greater delocalization of charges on this aromatic ring ligand compared with the more localized charge of the simple hydroxamate ligands.

Acknowledgment. This work was supported by the Director, Office of Energy Research, Office of Basic Energy Sciences, Chemical Sciences Division of the U.S. Department of Energy, under Contract No. DE-AC03-76SF00098. We thank Brandan Borgias for his assistance.

Registry No. $(C_5H_4NO_2)_4(H_2O)Th\cdot 2H_2O$, 86728-77-0; $(C_5H_4NO_2)_4Zr$, 86728-75-8; $(C_5H_4NO_2)_4Ce$, 86728-76-9; $(C_5H_4NO_2)_4U$, 86728-78-1.

Supplementary Material Available: Listings of anisotropic thermal parameters (Table IV), idealized hydrogen atom parameters (Table V), observed and calculated structure factor amplitudes (Table VI), and selected least-squares planes (Table VIII) (26 pages). Ordering information is given on any current masthead page.

Contribution No. 3098 from the Central Research and Development Department, Experimental Station, E.I. du Pont de Nemours and Company, Wilmington, Delaware 19898

NMR Spectra of Paramagnetic Group 8 Complexes of Bis(pyridylimino)isoindoline

PETER J. DOMAILLE, RICHARD L. HARLOW, STEVEN D. ITTEL,* and WILLIAM G. PEET

Received January 4, 1983

The susceptibility elements, χ_{ii}, of a series of transition-metal bis(2-pyridylimino)isoindoline (BPI) complexes have been determined by a solution-phase method based upon splittings observed in high-field, high-resolution deuterium NMR spectra. Details of the approach are discussed and applied to the interpretation of chemical shifts in the proton NMR spectra of the $M(BPI)_2$ complexes, M = Fe^{2+}, Co^{2+}, and Ni^{2+}. An X-ray crystal structure of bis(bis(3-methyl-2-pyridylimino)isoindolinato)manganese–methylene chloride (2/1) has been determined and combined with magnetic anisotropy data for the Co^{2+} complex to separate contact and dipolar contributions to the chemical shifts. ESR data and the method of isolated spins are compared with the deuterium quadrupole method of measuring the susceptibility elements in the cobalt complex. The crystal structure data at −100 °C are space group $P\bar{1}$, a = 9.643 (2) Å, b = 38.930 (9) Å, c = 9.539 (2) Å, α = 92.716 (2)°, β = 90.556 (2)°, γ = 86.574 (2)°, and Z = 4 for $Mn(C_{20}H_{16}N_5)_2 \cdot {}^1/_2CH_2Cl_2$, giving two independent molecules. The coordination geometry is octahedral with two meridional, three-coordinate, monoanionic ligands.

Introduction

The interpretation of the NMR spectra of paramagnetic molecules has received considerable attention in recent years.[1] One aspect of continuing focus is the requirement of clearly distinguishing the two independent contributions to the paramagnetic shift, the pseudocontact (dipolar) and contact terms. These individual contributions are separated by calculation of the dipolar shift from eq 1 and subtraction from

$$(\Delta H/H)_D = -\langle(3\cos^2\theta^* - 1)/3R^{*3}\rangle\Delta_\parallel\chi - \langle\sin^2\theta^*\cos 2\phi^*/2R^{*3}\rangle\Delta_\perp \quad (1a)$$

$$\Delta_\parallel\chi = (\chi_{zz} - {}^1/_2(\chi_{xx} + \chi_{yy})) \qquad \Delta_\perp\chi = (\chi_{xx} - \chi_{yy}) \quad (1b)$$

the measured isotropic shift.[1-5] Since a reasonable molecular geometry is usually available, (R^*, θ^*, ϕ^*) are calculable, while the difficult parameters to determine are the susceptibility elements, χ_{ii}.

Horrocks and co-workers[2] pioneered the use of single-crystal anisotropy measurements to determine the χ_{ii} values, while Jesson[3] and McGarvey[4] used low-temperature ESR measurements and ligand field calculations to derive the susceptibility anisotropy ($\Delta_\parallel\chi$) in axial molecules. The former method requires large single crystals with known projections of the molecular axes onto the crystallographic axes, while the latter approach needs detailed information about the excited

(1) (a) LaMar, G. N., Horrocks, W. D., Jr., Holm, R. H., Eds. "NMR of Paramagnetic Molecules"; Academic Press: New York, 1973. (b) Honeybourne, C. L. *Nucl. Magn. Reson. 6–8.*

(2) (a) Horrocks, W. D., Jr. *Inorg. Chem.* **1970**, *9*, 690–692. (b) Horrocks, W. D., Jr. Greenberg, E. S. *Ibid.* **1971**, *10*, 2190.

(3) (a) Jesson, J. P. *J. Chem. Phys.* **1966**, *45*, 1049–1056. (b) Jesson, J. P. *Ibid.* **1967**, *47*, 579–591.

(4) (a) Kurland, R. J.; McGarvey, B. R. *J. Magn. Reson.* **1970**, *2*, 286–301. (b) McGarvey, B. R. *J. Chem. Phys.* **1970**, *53*, 86–91.

(5) The octupolar contributions to the geometry-dependent shift are not expected to be significant in this case since R^* is approximately 5–8 Å for all protons except 6-pyridyl, which is 2.9 Å: (a) Stiles, P. J. *Mol. Phys.* **1975**, *29*, 1271. (b) Golding, R. M.; Pascual, R. O.; Stubbs, L. C. *Ibid.* **1976**, *31*, 1933. (c) Golding, R. M.; Pascual, R. O.; Vrbancich, J. *Ibid.* **1976**, *31*, 731.

0020-1669/83/1322-3944$01.50/0